How well do we characterize snow storage in High Mountain Asia?

Yufei Liu[1], Yiwen Fang[1], Dongyue Li[1] and Steven A. Margulis[1]

[1] Department of Civil and Environmental Engineering, University of California, Los Angeles, Los Angeles, CA, 90095.

Corresponding author: Steven A. Margulis (margulis@seas.ucla.edu)

Key Points:

- Existing snow products generally underestimate peak snow storage in High Mountain Asia compared with a novel snow reanalysis dataset
- Large inter-product variability in accumulation-season snowfall explains most of the uncertainty in peak snow storage
- Accumulation-season ablation plays a significant role in peak snow storage uncertainty and deserves more attention in future studies

Abstract

Accurate characterization of peak snow water storage in High Mountain Asia (HMA) is essential for assessing the water supply to over one billion downstream residents. Currently, such characterization still relies on modeling due to the measurement scarcity. Here, eight global snow products were examined over HMA using a newly developed High Mountain Asia Snow Reanalysis (HMASR) dataset as a reference. The focus of intercomparison was on peak annual snow storage, the first-order determinant of warm-season water availability in snow-dominated basins. Across eight products the climatological peak storage over HMA was found to be 161 km^3 $\pm$ 102 km^3 with an average 33% underestimation relative to HMASR. The inter-product variability in cumulative snowfall (335 km^3 $\pm$ 148 km^3) explains the majority (>80%) of peak snow storage uncertainty, while significant snowfall loss to ablation during accumulation season (51% $\pm$ 9%) also reveals the critical role of ablation processes on peak snow storage.

Plain Language Summary

Peak snow storage is important for summer and fall water availability in snow-dominated regions. Here, we evaluated the estimates of peak snow storage over High Mountain Asia (HMA) from eight global snow products with respect to the newly developed High Mountain Asia Snow Reanalysis (HMASR). The results suggest a large uncertainty and general underestimation (33%) in HMA-wide peak snow storage estimates across the global snow products, when compared to the reference HMASR. Inter-product snowfall variability among global snow products explains most of their peak snow storage uncertainty (over 80%). Significant snow ablation loss during the accumulation season (~50% of snowfall inputs) is also critical in contributing to the peak snow storage variations.

1 Introduction

Seasonal snow accumulation in global mountain "water towers" provides a virtual reservoir in winter that is essential for warm-season water supply (Viviroli et al., 2007). In High Mountain Asia (HMA), snowmelt feeds the major river basins (e.g. Indus, Amu Darya, Ganges) in their headwaters (Bookhagen and Burbank, 2010; Armstrong et al., 2019; Khanal et al., 2021; Kraaijenbrink et al., 2021), which is critical for meeting the human water demands of over 1 billion people in spring and summer (Immerzeel et al., 2010). Snow storage in seasonal snowpacks and the timing of snowmelt are highly sensitive to a warming climate, which is likely to alter the frequency of snow droughts (Huning and AghaKouchak, 2020) and pose risks to the water security for natural and human use (Immerzeel et al., 2020; Qin et al., 2020; Kraaijenbrink et al., 2021).

Snow water equivalent (SWE) is directly indicative of the total water resource availability in snowpacks at a given time. SWE reaches its seasonal peak at the end of the accumulation season (right before melt onset); accurately estimating peak snow storage (and its spatial distribution) is thus a first-order requirement for assessing snow-derived water availability for downstream use (Li et al., 2019). Despite its importance, the quantification of peak SWE over the world's mountains is still poorly constrained (Mudryk et al., 2015; Wrzesien et al., 2019), primarily due to the difficulties in directly measuring SWE, which is impeded by the scarcity or the non-existence of in situ gages in many critical regions and a lack of satellite-based remote sensing for globally consistent SWE measurements (Palazzi et al., 2013; Dozier et al., 2016; Bormann et al., 2018). SWE can be estimated through data assimilation and modeling approaches. However, previous intercomparison studies suggest large discrepancies in SWE estimation over the entire northern hemisphere (Mudryk et al., 2015; Mortimer et al., 2020; Xiao et al., 2020), North America or the Western United States (WUS; McCrary and Mearns, 2019; Wrzesien et al., 2019; Xu et al., 2019; Kim et al., 2021; Cho et al., 2022), Hindu Kush-Karakoram-Himalaya (Terzago et al., 2014), and the Tibetan Plateau (Bian et al., 2019; Orsolini et al., 2019). Despite the large uncertainties seen across the SWE products, studies assessing the links between snowpack storage, water availability and climate change are often based on a single snow dataset (e.g. Mankin et al., 2015; Huning and AghaKouchak, 2020; Immerzeel et al., 2020; Qin et al., 2020), which propagates the error in snow storage estimates to climatic and water resource availability quantification. Without improved characterization of seasonal snow storage, in regions like HMA, where the downstream regions have the densest population on Earth (over one billion residents in total) and the water supply to these residents heavily relies on snow-derived water, our confidence in estimating water resource availability and how it has been changing will remain compromised, thus impacting our ability to effectively adapt to ongoing changes.

In this study, the newly developed High Mountain Asia Snow Reanalysis (HMASR; Liu et al., 2021a, b) is employed as a reference SWE dataset to examine the peak snow storage estimates from eight global atmospheric reanalysis and land data assimilation products. The use of HMASR provides a new reference dataset, derived specifically for mountain domains and constrained by remote sensing observations, to perform a more thorough evaluation of snow storage estimates over the broad HMA domain. The focus herein is understanding the uncertainty in processes leading up to accumulation-season peak SWE storage due to its first-order determination of available water resources in snow-dominated regions. The novelty of this study is embedded in the answers to the following science questions:

1. What is the uncertainty in peak snow water storage over High Mountain Asia and its watersheds?

2. How much of the uncertainty in peak snow storage is explained by the variability in accumulation-season snowfall and ablation, respectively?

2 Data

Herein the reference SWE dataset (HMASR) and eight reanalysis datasets are examined. The eight global datasets (Text S1 and Table S1) are chosen as representative community-based global products that span most of the period of HMASR (1999-2017), including: ERA5 and ERA5-land (European Centre for Medium-Range Weather Forecasts (ECMWF) Re-Analysis products, 5th generation; Hersbach et al., 2020; Muñoz-Sabater et al., 2021), MERRA2 (Modern-Era Retrospective analysis for Research and Applications, version 2; Gelaro et al., 2017), JRA55 (Japanese 55-year Reanalysis; Kobayashi et al., 2015) and four GLDAS-2.1 products (Global Land Data Assimilation System version 2.1; Rodell et al., 2004) at several resolutions and with different land surface models (GLDAS-Noah (0.25°), GLDAS-Noah (1°), GLDAS-VIC (1°), and GLDAS-CLSM (1°), details listed in Table S1). Hereafter, to distinguish the globally-available datasets and the reference dataset, we use "snow products" and "HMASR" respectively.

The intercomparison study period is chosen as Water Years (WYs) 2001 to 2017, with the maximum overlap across all datasets (Table S1; with WY 2001 spanning from 1 October 2000 to 30 September 2001 for example). All nine datasets provide SWE estimates to evaluate the peak seasonal water storage. Other meteorological forcings (precipitation, P; air temperature, T_a; and snowfall, S) are obtained from the global snow products. HMASR (which does not include snowfall) provides only SWE for comparison. The meteorological forcing variables for each snow product are obtained at their raw spatial and temporal resolutions (Table S1) and are aggregated into daily total values (for P and S) or daily average values (for T_a). Spatial aggregation is also performed for SWE and meteorological forcings to facilitate the intercomparison and the analysis at the basin- or domain-scale (Sections 4.1).

3 Study region and Methods

3.1 Study domain and classification of seasonal, ephemeral, and persistent snow regions

The HMA region (Figure 1a) includes key mountain ranges (e.g. Tien Shan, Pamir, Karakoram, Himalayas, etc.) and the Tibetan Plateau. Westerlies dominate winter precipitation in the northwest and the Indian and East Asia monsoons dominate summer precipitation in the southeast (Yao et al., 2012).

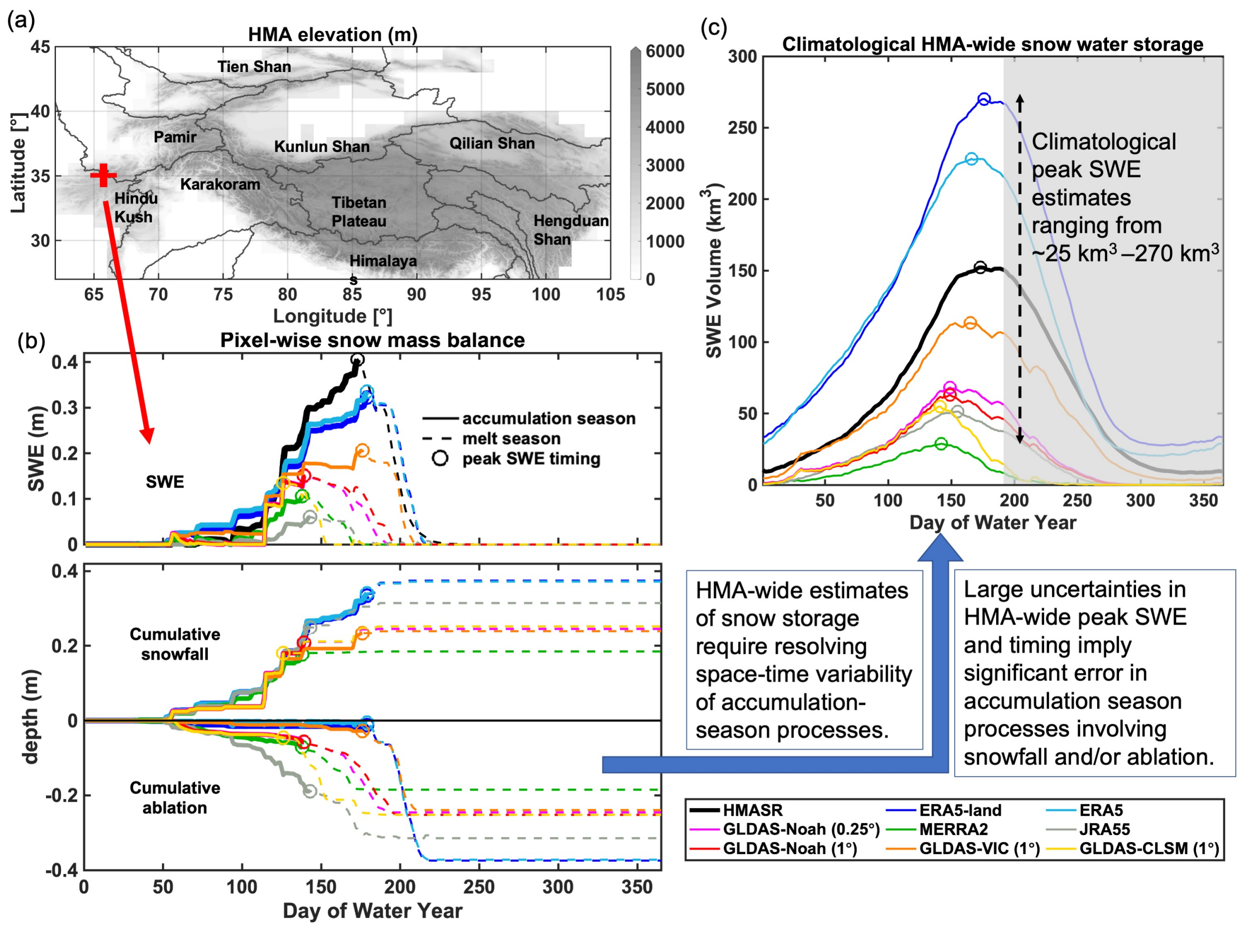

Figure 1. **a**) map of HMASR domain elevation with major watershed boundaries. The red '+' symbol indicates the location shown in (b); **b**) an illustrative example of the seasonal cycle of SWE, cumulative snowfall, and cumulative ablation at a representative pixel in WY2017. The solid curves represent processes leading up to peak SWE (the focus of the work described herein), and the dashed curves represent the processes after peak SWE. The 'o' symbols on the curves

indicate peak SWE timing; **c**) the 17-year climatology of the seasonal cycle of HMA-wide SWE volume. The colors of the curves in (**b**) and (**c**) represent the estimation from different datasets.

3.2 Accumulation-season snow mass balance

Snowpack evolution can be characterized as snow mass gain (via solid precipitation, i.e. snowfall) and snow mass loss (via ablation, e.g. snowmelt, sublimation, wind drifting, etc.), which can be represented with mass and energy balance (Liston and Elder, 2006; McCrary and Mearns, 2019). Herein we only focus on accumulation-season processes, as accurately characterizing peak storage is a necessary condition for accurately representing ablation-season processes and the total snowmelt water resource availability.

We start with defining the snow accumulation season at the pixel-scale (from day of water year (DOWY) 1 until pixel-wise peak SWE DOWY, Text S2 and Figure S1). Note that ‘accumulation season’ is most robustly defined for seasonal snow rather than ephemeral snow, as the latter is intermittent, where snow may accumulate and fully disappear multiple times within a WY (Petersky and Harpold, 2018). Both seasonal and ephemeral snow are important types (Sturm et al. 1995), while the former is more critical for water supply and thus emphasized in this work. Through the snow mass balance within the accumulation season (Text S3), we obtain the relationship:

$$swe_{peak} = s_{acc} - a_{acc} \tag{1}$$

where swe_{peak} is the pixel-wise peak SWE, and s_{acc} and a_{acc} respectively denote the cumulative snowfall and snow ablation integrated over the accumulation season.

In this work, both swe_{peak} and s_{acc} are obtained from the snow products, and a_{acc} is computed as the difference between s_{acc} and swe_{peak} (Text S3). Figure 1b provides an illustrative example showing the seasonal cycle of SWE, cumulative snowfall and ablation at a representative pixel in WY2017, showing clear differences in swe_{peak} and its timing across products. Note that this comparison is primarily for illustration due to the large grid size differences among datasets. We also provide the caveat in using JRA55 that the diagnosed a_{acc} is likely a mix of model-specific ablation processes and non-negligible data assimilation corrections (Text S3).

The focus of this study is to quantitatively compare the seasonal snow storage estimates over the full HMA domain and at subregional scales through integrating pixel-scale quantities into basin- or HMA-scale volumes. Herein the 10 largest watersheds in HMA are examined (Lehner et al., 2008) and shown in Figure 1a. Seasonal, ephemeral, and persistent snow masks (Figure S2; Table S2; Text S4) are applied prior to the integration, with persistent snow excluded in the volume integration. For the three quantities in equation (1), the spatially integrated volumes are denoted herein as SWE_{peak}, S_{acc} and A_{acc} (in units of km^3), with the same relationship:

$$SWE_{peak} = S_{acc} - A_{acc} \tag{2}$$

It should be noted that A_{acc} is calculated as the difference between S_{acc} and SWE_{peak} as noted earlier. Spatial integration over elevation bands (using intervals of 1000 m) is also performed in this work (Text S5; Figure S3).

The analysis presented in this work consists of examining SWE_{peak} across all datasets (including using HMASR as a reference) and additionally S_{acc} and A_{acc} across all snow products.

More specifically, a linear regression (Text S6) is applied to examine the variations in S_{acc} loss to A_{acc} and their ability to explain SWE_{peak} variance:

$$SWE_{peak} = \beta * S_{acc} + \varepsilon \tag{3}$$

where β is the regression coefficient (slope), and ε is the random noise. SWE_{peak} and S_{acc} are obtained from each product and for each WY. Note that JRA55 and HMASR data were excluded in the linear regression, since their snowfall data is either not available (HMASR) or inconsistent with SWE (JRA55, due to significant data assimilation corrections in SWE; Text S3).

4 Results and Discussion

4.1 Uncertainty in peak snow storage over HMA and its watersheds

4.1.1 HMA-scale

The integrated SWE volume climatology (17-year average) time series over HMA (Figure 1c) shows significant variations in peak storage (a range of ~240 km^3) and peak timing (a range of ~35 days). Among these snow products, the largest peak snow storage is an order of magnitude greater than the lowest storage, and the earliest peak timing is one month ahead of the latest, suggesting large uncertainty across snow products. To better understand what drives the HMA-wide storage differences and isolate accumulation-season sources of uncertainty, all results to follow focus on the pixel-wise peak snow storage (SWE_{peak}) and the processes leading to that storage (S_{acc} and A_{acc}).

The climatological HMA-wide SWE_{peak}(pixel-wise peak snow storage) estimate is 161 km^3 $\pm$ 102 km^3 across all global snow products (with HMASR as a standalone dataset for evaluation; Text S7 and Table S3), exhibiting a 63% uncertainty relative to the mean. When partitioned into seasonal and ephemeral snow, the estimates are 110 km^3 $\pm$ 74 km^3 and 51 km^3 $\pm$ 28 km^3, respectively. The ERA5-land and ERA5 snow products, with volumes of 341 km^3 and 288 km^3, exhibit larger values than HMASR (239 km^3), corresponding to 43% and 20% more snow respectively. The GLDAS estimates all exhibit less snow than HMASR, with estimates of GLDAS-VIC (179 km^3), GLDAS-Noah (120 km^3 and 114 km^3 for 0.25° and 1° respectively), and GLDAS-CLSM (98 km^3), corresponding to 25%, 50%, 53% and 59% less snow than HMASR. The JRA55 and MERRA2 products exhibit the lowest SWE_{peak} with 93 km^3 (61% less than HMASR) and 54 km^3 (77% less than HMASR), respectively. When the snow products are compared collectively to HMASR over the full HMA domain, the mean difference (MD) in SWE_{peak} is -33% with a root mean square difference (RMSD) of 52%. In seasonal snow regimes, there is a MD of -47% and RMSD of 58%. In ephemeral snow regimes, there is a MD of 70% and RMSD of 113%. This highlights the qualitative differences across snow regimes (underestimation in seasonal vs. overestimation in ephemeral) that are partially canceled out when considered together.

4.1.2 Basin-scale

Coherent spatial patterns in swe_{peak} climatology are observed in all datasets (Figure 2a), which is consistent with previous work (e.g. Bian et al., 2019 and Orsolini et al, 2019). However, pixel-wise swe_{peak} magnitudes vary significantly across datasets (Figure 2a), so do the basin-integrated volumes (SWE_{peak}; Figure 2b). ERA5 and ERA5-land exhibit the highest SWE_{peak} values in all basins over HMA. These products have the best agreement with the HMASR estimates in the winter westerly-dominated basins (Syr Darya, Amu Darya, and Indus), where the other products all underestimate SWE_{peak} compared to HMASR. MERRA2 consistently shows the least SWE_{peak} across all basins.

In contrast, SWE_{peak} is significantly overestimated in ERA5 and ERA5-land, compared to HMASR, in the monsoon-dominated basins (Salween, Mekong, Yangtze and Yellow), which may be caused by the excess precipitation and lack of melt in its snow model (Orsolini et al., 2019; Hersbach et al., 2020). GLDAS products show the best agreement with HMASR in these basins, followed by JRA55 with comparable or slightly underestimated SWE_{peak} values. This is not surprising as JRA55 assimilates in-situ snow depth observations over the Tibetan Plateau, where most stations are sparsely located in the valleys over the eastern HMA (Bian et al., 2019). As suggested in previous work, JRA55 and GLDAS products have relatively good performance in estimating SWE/snow depth compared to in-situ data (Bian et al., 2019; Orsolini et al., 2019; Wang et al., 2020).

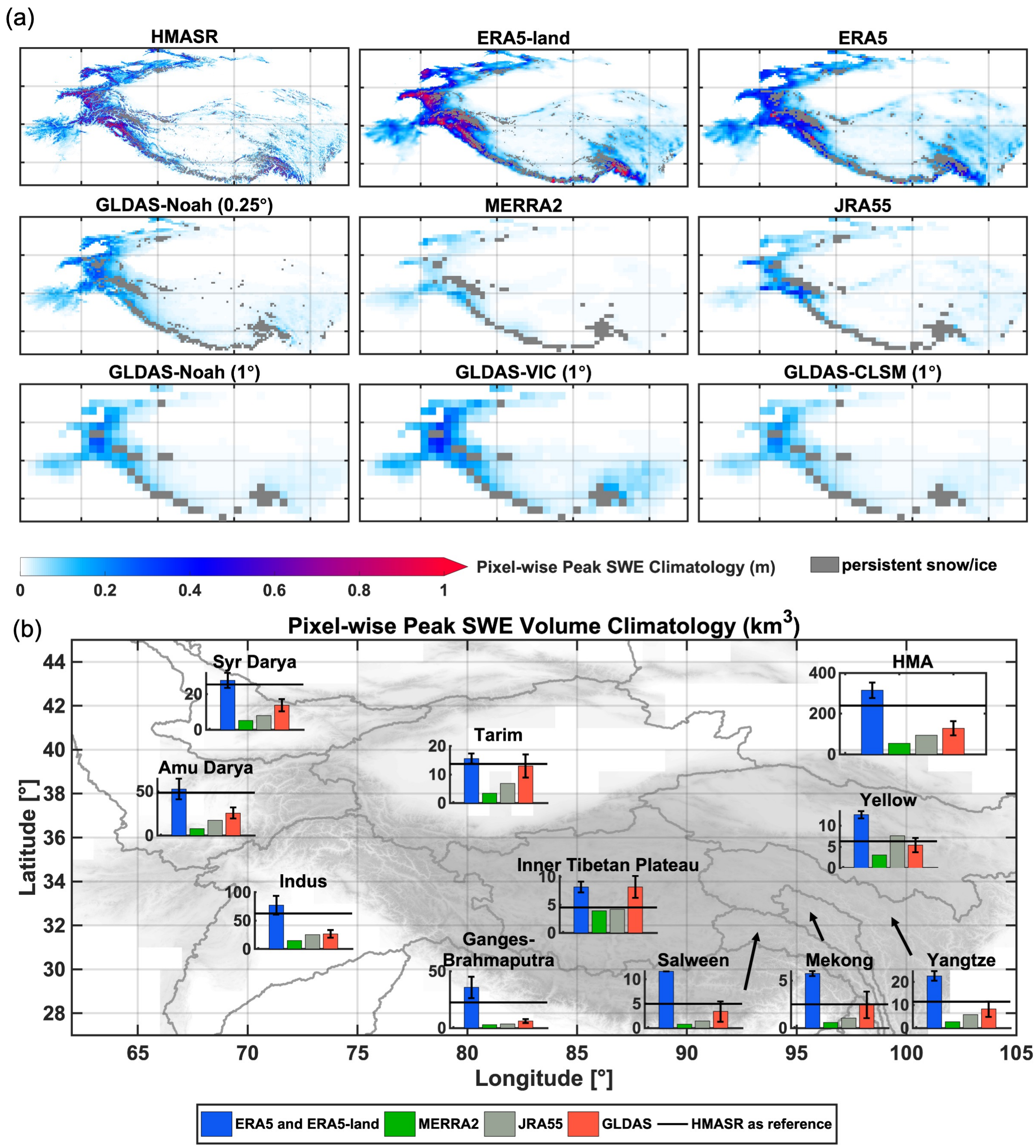

Figure 2. a) The 17-year climatology of pixel-wise peak SWE (swe_{peak}), with persistent snow/ice pixels masked out (gray); **b**) The 17-year climatology of peak SWE volume in each basin (SWE_{peak}, with HMASR SWE shown with horizontal black line). The snow products are grouped into 4 main sets (ERA5 and ERA5-land, MERRA2, JRA55 and GLDAS), with the average SWE_{peak} (bar plot) and the standard deviation (error bars) shown for the ERA5 and GLDAS groups.

4.2 Drivers of peak SWE variations across snow products

4.2.1 Accumulation-season snowfall and ablation

The variability in S_{acc} and A_{acc} climatology among snow products is characterized in Figure 3 to illustrate their relative influence on SWE_{peak} variability. Overall, there exists large variations in S_{acc} and A_{acc} estimates across the existing snow products. S_{acc} is generally the largest in ERA5/ERA5-land products and is the smallest in MERRA2/GLDAS products, with the mean and uncertainty characterized by 335 km^3 $\pm$ 148 km^3 over the entire HMA, 178 km^3 $\pm$ 83 km^3 in seasonal snow regimes and 157 km^3 $\pm$ 67 km^3 in ephemeral snow regimes. A_{acc} and its ratio to S_{acc} are also quite significant and variable across snow products, indicating snow loss via ablation during the accumulation season is a non-negligible factor in determining SWE_{peak}. Specifically, between 40% (ERA5-land) and 65% (MERRA2) of snowfall is lost to ablation during the accumulation season, with the overall ablation loss fraction given by 51% $\pm$ 9%. The snowfall loss to ablation is less in seasonal snow regimes, but the ratio still varies significantly across products (from 17% in ERA5-land to 55% in MERRA2, or 37% $\pm$ 13% across snow products). In ephemeral snow regimes, the snowfall loss to ablation during the accumulation season is large but more consistent across snow products (from 58% in GLDAS-VIC to 76% in MERRA2; 67% $\pm$ 7%). Other work, focused on the WUS has also identified ablation as a significant accumulation-season loss term (Cho et al., 2022).

The elevational distribution of S_{acc}, A_{acc} and SWE_{peak} climatology over the full HMA domain were normalized by total S_{acc} volume to illustrate the volumetric fraction (Figure S4). The distribution in fractional S_{acc} exhibits general consistency across snow products, while the distribution in fractional A_{acc} is significantly more distinct across products. This leads to a distinct distribution in fractional SWE_{peak} rather than just reproducing the fractional S_{acc} distribution, and highlights the important role of ablation in removing snowfall differently with elevation over the accumulation season (Text S8).

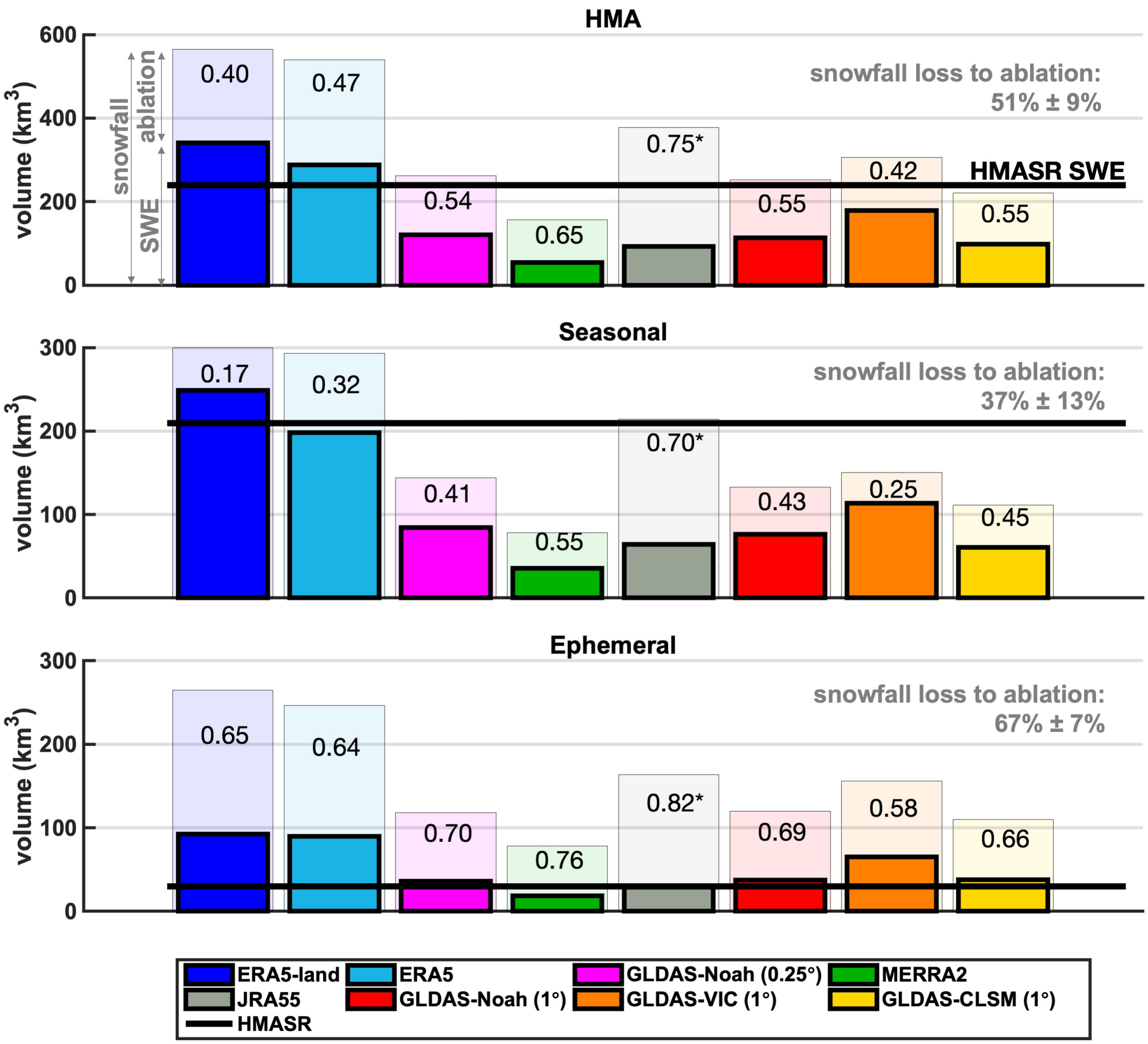

Figure 3. The 17-year climatology of peak SWE volume (SWE_{peak}, solid bars) and accumulation-season snowfall volume (S_{acc}, shaded bars) integrated over HMA (top panel) and areas with seasonal (middle panel) and ephemeral snow (bottom panel). HMASR SWE is provided as a reference (solid black horizontal line). The text labels in each bar plot indicate the fraction of cumulative accumulation-season snowfall lost to ablation. JRA55 ablation fraction is only displayed here (noted with a symbol *) but not included in the discussion due to its diagnosed ablation being overestimated as a result of its snow data assimilation updates (Text S3).

4.2.2 Contributions to peak snow storage variations

To explain peak SWE variations, linear regression (Text S6) was applied across snow products and/or WYs. Over the full HMA domain, a strong linear dependence between the interannual SWE_{peak} and S_{acc} is clear (Figure 4a). Notably, S_{acc} values exhibit a large range (100 – 700 km^3) and have a sizeable gap between GLDAS and ERA5/ERA5-land. The global regression slope (β_{global}; across all snow products) is 0.54, indicating that, during the accumulation season, ~54% of snowfall goes into SWE_{peak}, while the other 46% is lost through ablation. Snowfall's contribution to SWE_{peak} is higher in seasonal snow regimes (Figure 4b), where ~71% of snowfall goes into peak SWE and 29% is lost via ablation. In ephemeral snow regimes (Figure 4c), however, ~35% of snowfall goes into peak SWE while 65% is lost via ablation. These diagnosed fractions from multi-WY and multi-product analysis (Figure 4) are consistent with those derived from the climatology (Figure 3). The coefficient of determination (R^2) is 0.88, 0.88 and 0.80 for the full HMA domain, seasonal snow regime and ephemeral snow regime, respectively. Such values are informative in 1) confirming the expected strong linear dependence of SWE_{peak} and S_{acc} across all datasets and all WYs, and 2) over 80% of SWE_{peak} uncertainty is explained by S_{acc} variability and the other 20% or less is explained by A_{acc} variations.

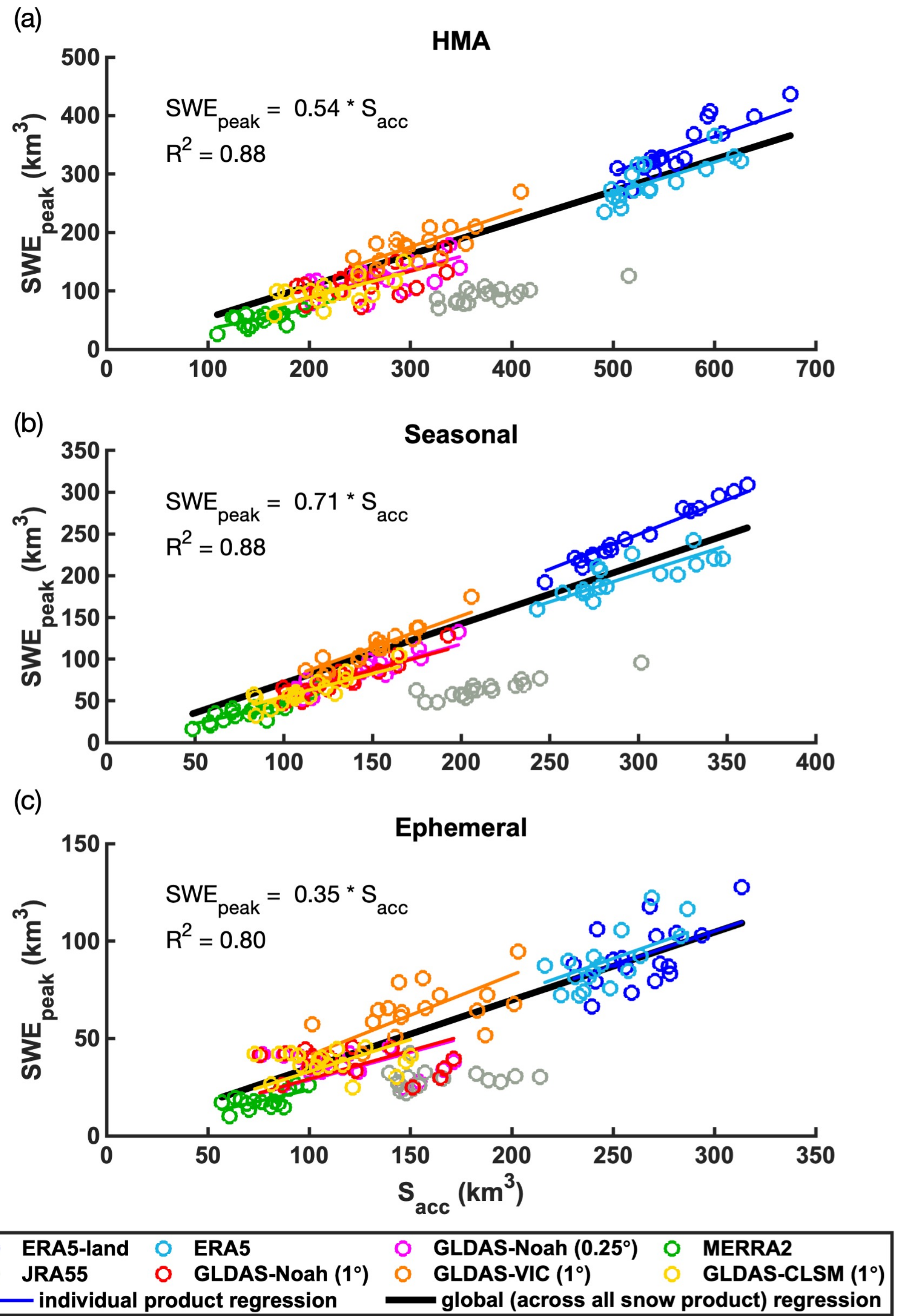

Figure 4. Regression of peak SWE volume (SWE_{peak}) and accumulation-season snowfall (S_{acc}) across all WYs (2001-2017), with volumes integrated over the **a)** the full HMA domain, **b)** seasonal, and **c)** ephemeral snow regimes, respectively. Note that JRA55 is displayed here but is not included in the linear regression due to its diagnosed ablation being overestimated as a result of its snow data assimilation updates.

In addition to treating all datasets as a large sample, we also evaluated the interannual variability for individual snow products and examined product-specific linear regression results. The individual regression slopes are distinct from the global slope value (Figure 4 and Table S4). ERA5-land and GLDAS-VIC exhibit higher slopes, while MERRA2 and the other GLDAS products exhibit lower slopes. The linear dependence of SWE_{peak} and S_{acc} are very strong in seasonal snow (with R^2 ranging from 0.62 to 0.94) but much weaker in ephemeral snow (with R^2 ranging from 0.25 to 0.48) when examining individual snow products (Text S9 and Table S4). This can be attributed to ephemeral snow being more influenced by ablation, introducing additional noise into the snowfall-peak SWE relationship.

Given the large range in S_{acc} across snow products, including the sizeable gap between ERA5/ERA5-land and the other snow products (GLDAS and MERRA2), we also separately regressed SWE_{peak} vs. S_{acc} for these two groups of snow products (Text S9 and Figure S5). In doing so, the R^2 values drop to 58% and 43% respectively (from the global value of 0.88), indicating that A_{acc} is a more important (explaining 42% and 57% of SWE_{peak} uncertainty, respectively) when examined in certain subsets of products.

The results above indicate (not surprisingly) that S_{acc} variations are the primary factor in explaining SWE_{peak} variations in HMA, while ablation plays an important role. To decipher the degree to which those variations are explained by variations in precipitation vs. rain-snow partitioning across snow products, the accumulation-season snowfall volume (S_{acc}) was regressed against precipitation volume (P_{acc}) (Text S9 and Figure S6). S_{acc} shows very high linear dependence on P_{acc} (R^2 up to 0.96), and there is a relatively minor difference when adding accumulation-season air temperature into the regression (R^2 slightly increased to ~0.98). This identifies the key role of precipitation in contributing to SWE_{peak} uncertainties (where similar results are found in Cho et al., 2022 in the WUS), highlighting the top priority of reducing precipitation uncertainties for accurate SWE estimation.

5 Conclusion

Accurate knowledge of peak snow water storage in HMA is a pre-requisite for predicting warm-season runoff, which is critical for the water supply to the large population and agricultural production in downstream areas. Results in this study confirm that our current state of knowledge of this important water resource is highly uncertain. Eight globally available snow products were examined, with the use of HMASR as a reference, to specifically analyze the peak snow storage and how it is affected by accumulation vs. ablation processes during the accumulation season. The key findings are:

1) The integrated pixel-wise peak snow storage (SWE_{peak}) climatology across snow products was found to be 161 km^3 $\pm$ 102 km^3 over HMA, with varying uncertainty levels for seasonal (110 km^3 $\pm$ 74 km^3) vs. ephemeral (51 km^3 $\pm$ 28 km^3) snow. Compared to HMASR, the other snow products on average underestimate SWE_{peak} by 33% (MD) with a RMSD of 52% over the entire HMA. The error and uncertainty vary across different watersheds, where on average, the snow products underestimate seasonal snow (by 47%) and overestimate ephemeral snow (by 70%), compared to HMASR.

2) There exists large variability in the accumulation-season snowfall (S_{acc}) and ablation (A_{acc}) climatology. S_{acc} climatology was found to be 335 km^3 $\pm$ 148 km^3, with 51% $\pm$

9% of the total accumulation-season snowfall lost via ablation prior to the peak snow timing. The fraction differs between seasonal (37% $\pm$ 13%) and ephemeral (67% $\pm$ 7%) snow regimes. Both S_{acc} and A_{acc} play important roles in determining the spatial and elevational distribution in SWE_{peak}.

3) Uncertainty in inter-product peak snow storage estimates over HMA is primarily explained by S_{acc} (88%), with 88% and 80% in seasonal and ephemeral snow regimes respectively. The sensitivity to the chosen snow product ensemble could be a caveat to the relative importance of S_{acc} in explaining SWE_{peak} uncertainty; when the eight datasets are partitioned into two subsets (as separated by the notable gap in S_{acc}), A_{acc} was found to explain more SWE_{peak} variations (42% and 57%, respectively) when examined within each subset.

Reducing accumulation-season uncertainty will be a key first step to properly constraining melt-season processes (i.e. by providing an accurate initial condition of stored snow) that control snowmelt rates, infiltration, and runoff. Reducing the uncertainty in HMA snow storage estimates will require improved characterization of both snowfall and ablation processes and/or better measurements of SWE to constrain models during the accumulation season. The specific drivers for snow ablation variability during the accumulation season are not explored in this work, as they are typically intertwined with individual model physics, but are also important for peak SWE estimation (Cho et al., 2022) and should be investigated in future work.

Acknowledgments

We would like to thank those responsible for the creation of the datasets used in this study. This research was funded by the NASA High-Mountain Asia Program Grant #NNX16AQ63G with additional support provided by NSF Grant #1641960.

Open Research

Data Availability Statement

The HMASR dataset used in this work is publicly available on National Snow and Ice Data Center (NSIDC; https://doi.org/10.5067/HNAUGJQXSCVU). Other global reanalysis products are also acquired online: ERA5 and ERA5-land data are obtained from the Copernicus Climate Change Service (C3S) Climate Date Store (ERA5: https://doi.org/10.24381/cds.adbb2d47; ERA5-land: https://doi.org/10.24381/cds.e2161bac). JRA55 is downloaded from: http://search.diasjp.net/en/dataset/JRA55.

MERRA2 data is obtained from the NASA Goddard Earth Sciences Data and Information Service Center (GES DISC; https://disc.gsfc.nasa.gov/), with the specification of SWE (SNOMAS) obtained from https://doi.org/10.5067/RKPHT8KC1Y1T, bias-corrected precipitation (PRECTOTCORR) obtained from https://doi.org/10.5067/7MCPBJ41Y0K6, bias-corrected snowfall (PRECSNOCORR) from https://doi.org/10.5067/L0T5GEG1NYFA, air temperature (T2M) from https://doi.org/10.5067/VJAFPLI1CSIV.

GLDAS datasets are also obtained from GES DISC (GLDAS-2.1 version is used in this work), as follows: GLDAS-Noah (0.25°) is acquired from https://doi.org/10.5067/E7TYRXPJKWOQ; GLDAS-Noah (1°) is acquired from https://doi.org/10.5067/IIG8FHR17DA9; GLDAS-VIC (1°) is acquired from https://doi.org/10.5067/ZOG6BCSE26HV; and GLDAS-CLSM (1°) is acquired from https://doi.org/10.5067/VCO8OCV72XO0.

References

Armstrong, R. L., Rittger, K., Brodzik, M. J., Racoviteanu, A., Barrett, A. P., Khalsa, S.-J. S., Raup, B., Hill, A. F., Khan, A. L., Wilson, A. M., Kayastha, R. B., Fetterer, F., & Armstrong, B. (2019). Runoff from glacier ice and seasonal snow in High Asia: Separating melt water sources in river flow. *Regional Environmental Change*, *19*(5), 1249–1261. https://doi.org/10.1007/s10113-018-1429-0

Bian, Q., Xu, Z., Zhao, L., Zhang, Y.-F., Zheng, H., Shi, C., Zhang, S., Xie, C., & Yang, Z.-L. (2019). Evaluation and Intercomparison of Multiple Snow Water Equivalent Products over the Tibetan Plateau. *Journal of Hydrometeorology*, *20*(10), 2043–2055. https://doi.org/10.1175/JHM-D-19-0011.1

Bookhagen, B., & Burbank, D. W. (2010). Toward a complete Himalayan hydrological budget: Spatiotemporal distribution of snowmelt and rainfall and their impact on river discharge. *Journal of Geophysical Research: Earth Surface*, *115*(F3). https://doi.org/10.1029/2009JF001426

Bormann, K. J., Brown, R. D., Derksen, C., & Painter, T. H. (2018). Estimating snow-cover trends from space. *Nature Climate Change*, *8*(11), 924–928. https://doi.org/10.1038/s41558-018-0318-3

Cho, E., Vuyovich, C. M., Kumar, S. V., Wrzesien, M. L., Kim, R. S., & Jacobs, J. M. (2022). Precipitation Biases and Snow Physics Limitations Drive the Uncertainties in Macroscale Modeled Snow Water Equivalent. *Hydrology and Earth System Sciences Discussions*, *2022*, 1–22. https://doi.org/10.5194/hess-2022-136

Dozier, J., Bair, E. H., & Davis, R. E. (2016). Estimating the spatial distribution of snow water equivalent in the world's mountains. *WIREs Water*, *3*(3), 461–474. https://doi.org/10.1002/wat2.1140

Gelaro, R., McCarty, W., Suárez, M. J., Todling, R., Molod, A., Takacs, L., Randles, C. A., Darmenov, A., Bosilovich, M. G., Reichle, R., Wargan, K., Coy, L., Cullather, R., Draper, C., Akella, S., Buchard, V., Conaty, A., da Silva, A. M., Gu, W., … Zhao, B. (2017). The Modern-Era Retrospective Analysis for Research and Applications, Version 2 (MERRA-2). *Journal of Climate*, *30*(14), 5419–5454. https://doi.org/10.1175/JCLI-D-16-0758.1

Hersbach, H., Bell, B., Berrisford, P., Hirahara, S., Horányi, A., Muñoz-Sabater, J., Nicolas, J., Peubey, C., Radu, R., Schepers, D., Simmons, A., Soci, C., Abdalla, S., Abellan, X., Balsamo, G., Bechtold, P., Biavati, G., Bidlot, J., Bonavita, M., … Thépaut, J.-N. (2020).

The ERA5 global reanalysis. *Quarterly Journal of the Royal Meteorological Society*, *146*(730), 1999–2049. https://doi.org/10.1002/qj.3803

Huning, L. S., & AghaKouchak, A. (2020). Global snow drought hot spots and characteristics. *Proceedings of the National Academy of Sciences*, *117*(33), 19753. https://doi.org/10.1073/pnas.1915921117

Immerzeel, W. W., Lutz, A. F., Andrade, M., Bahl, A., Biemans, H., Bolch, T., Hyde, S., Brumby, S., Davies, B. J., Elmore, A. C., Emmer, A., Feng, M., Fernández, A., Haritashya, U., Kargel, J. S., Koppes, M., Kraaijenbrink, P. D. A., Kulkarni, A. V., Mayewski, P. A., … Baillie, J. E. M. (2020). Importance and vulnerability of the world's water towers. *Nature*, *577*(7790), 364–369. https://doi.org/10.1038/s41586-019-1822-y

Immerzeel, W. W., van Beek, L. P. H., & Bierkens, M. F. P. (2010). Climate Change Will Affect the Asian Water Towers. *Science*, *328*(5984), 1382. https://doi.org/10.1126/science.1183188

Khanal, S., Lutz, A. F., Kraaijenbrink, P. D. A., van den Hurk, B., Yao, T., & Immerzeel, W. W. (2021). Variable 21st Century Climate Change Response for Rivers in High Mountain Asia at Seasonal to Decadal Time Scales. *Water Resources Research*, *57*(5), e2020WR029266. https://doi.org/10.1029/2020WR029266

Kim, R. S., Kumar, S., Vuyovich, C., Houser, P., Lundquist, J., Mudryk, L., Durand, M., Barros, A., Kim, E. J., Forman, B. A., Gutmann, E. D., Wrzesien, M. L., Garnaud, C., Sandells, M., Marshall, H.-P., Cristea, N., Pflug, J. M., Johnston, J., Cao, Y., … Wang, S. (2021). Snow Ensemble Uncertainty Project (SEUP): Quantification of snow water equivalent uncertainty across North America via ensemble land surface modeling. *The Cryosphere*, *15*(2), 771–791. https://doi.org/10.5194/tc-15-771-2021

KOBAYASHI, S., OTA, Y., HARADA, Y., EBITA, A., MORIYA, M., ONODA, H., ONOGI, K., KAMAHORI, H., KOBAYASHI, C., ENDO, H., MIYAOKA, K., & TAKAHASHI, K. (2015). The JRA-55 Reanalysis: General Specifications and Basic Characteristics. *Journal of the Meteorological Society of Japan. Ser. II*, *93*(1), 5–48. https://doi.org/10.2151/jmsj.2015-001

Kraaijenbrink, P. D. A., Stigter, E. E., Yao, T., & Immerzeel, W. W. (2021). Climate change decisive for Asia's snow meltwater supply. *Nature Climate Change*, *11*(7), 591–597. https://doi.org/10.1038/s41558-021-01074-x

Lehner, B., Verdin, K., & Jarvis, A. (2008). New Global Hydrography Derived From Spaceborne Elevation Data. *Eos, Transactions American Geophysical Union*, *89*(10), 93–94. https://doi.org/10.1029/2008EO100001

Li, D., Lettenmaier, D. P., Margulis, S. A., & Andreadis, K. (2019). The Value of Accurate High-Resolution and Spatially Continuous Snow Information to Streamflow Forecasts. *Journal of Hydrometeorology*, *20*(4), 731–749. https://doi.org/10.1175/JHM-D-18-0210.1

Liston, G. E., & Elder, K. (2006). A Distributed Snow-Evolution Modeling System (SnowModel). *Journal of Hydrometeorology*, *7*(6), 1259–1276. https://doi.org/10.1175/JHM548.1

Liu, Y., Fang, Y., & Margulis, S.A. (2021a). High Mountain Asia UCLA Daily Snow Reanalysis, Version 1. Boulder, Colorado USA, NASA Snow and Ice Data Center Distributed Active Archive Center. https://doi.org/10.5067/HNAUGJQXSCVU

Liu, Y., Fang, Y., & Margulis, S. A. (2021b). Spatiotemporal distribution of seasonal snow water equivalent in High Mountain Asia from an 18-year Landsat–MODIS era snow reanalysis dataset. *The Cryosphere*, *15*(11), 5261–5280. https://doi.org/10.5194/tc-15-5261-2021

Mankin, J. S., Viviroli, D., Singh, D., Hoekstra, A. Y., & Diffenbaugh, N. S. (2015). The potential for snow to supply human water demand in the present and future. *Environmental Research Letters*, *10*(11), 114016. https://doi.org/10.1088/1748-9326/10/11/114016

McCrary, R. R., & Mearns, L. O. (2019). Quantifying and Diagnosing Sources of Uncertainty in Midcentury Changes in North American Snowpack from NARCCAP. *Journal of Hydrometeorology*, *20*(11), 2229–2252. https://doi.org/10.1175/JHM-D-18-0248.1

Mortimer, C., Mudryk, L., Derksen, C., Luojus, K., Brown, R., Kelly, R., & Tedesco, M. (2020). Evaluation of long-term Northern Hemisphere snow water equivalent products. *The Cryosphere*, *14*(5), 1579–1594. https://doi.org/10.5194/tc-14-1579-2020

Mudryk, L. R., Derksen, C., Kushner, P. J., & Brown, R. (2015). Characterization of Northern Hemisphere Snow Water Equivalent Datasets, 1981–2010. *Journal of Climate*, *28*(20), 8037–8051. https://doi.org/10.1175/JCLI-D-15-0229.1

Muñoz-Sabater, J., Dutra, E., Agustí-Panareda, A., Albergel, C., Arduini, G., Balsamo, G., Boussetta, S., Choulga, M., Harrigan, S., Hersbach, H., Martens, B., Miralles, D. G., Piles, M., Rodríguez-Fernández, N. J., Zsoter, E., Buontempo, C., & Thépaut, J.-N. (2021). ERA5-Land: A state-of-the-art global reanalysis dataset for land applications. *Earth System Science Data*, *13*(9), 4349–4383. https://doi.org/10.5194/essd-13-4349-2021

Orsolini, Y., Wegmann, M., Dutra, E., Liu, B., Balsamo, G., Yang, K., de Rosnay, P., Zhu, C., Wang, W., Senan, R., & Arduini, G. (2019). Evaluation of snow depth and snow cover over the Tibetan Plateau in global reanalyses using in situ and satellite remote sensing observations. *The Cryosphere*, *13*(8), 2221–2239. https://doi.org/10.5194/tc-13-2221-2019

Palazzi, E., Hardenberg, J., & Provenzale, A. (2013). Precipitation in the Hindu-Kush Karakoram Himalaya: Observations and future scenarios. *Journal of Geophysical Research: Atmospheres*, *118*(1), 85–100. https://doi.org/10.1029/2012JD018697

Petersky, R., & Harpold, A. (2018). Now you see it, now you don't: A case study of ephemeral snowpacks and soil moisture response in the Great Basin, USA. *Hydrology and Earth System Sciences*, *22*(9), 4891–4906. https://doi.org/10.5194/hess-22-4891-2018

Qin, Y., Abatzoglou, J. T., Siebert, S., Huning, L. S., AghaKouchak, A., Mankin, J. S., Hong, C., Tong, D., Davis, S. J., & Mueller, N. D. (2020). Agricultural risks from changing snowmelt. *Nature Climate Change*, *10*(5), 459–465. https://doi.org/10.1038/s41558-020-0746-8

Rodell, M., Houser, P. R., Jambor, U., Gottschalck, J., Mitchell, K., Meng, C.-J., Arsenault, K., Cosgrove, B., Radakovich, J., Bosilovich, M., Entin, J. K., Walker, J. P., Lohmann, D., & Toll, D. (2004). The Global Land Data Assimilation System. *Bulletin of the American Meteorological Society*, *85*(3), 381–394. https://doi.org/10.1175/BAMS-85-3-381

Sturm, M., Holmgren, J., & Liston, G. E. (1995). A Seasonal Snow Cover Classification System for Local to Global Applications. *Journal of Climate*, *8*(5), 1261–1283. https://doi.org/10.1175/1520-0442(1995)008<1261:ASSCCS>2.0.CO;2

Terzago, S., von Hardenberg, J., Palazzi, E., & Provenzale, A. (2014). Snowpack Changes in the Hindu Kush–Karakoram–Himalaya from CMIP5 Global Climate Models. *Journal of Hydrometeorology*, *15*(6), 2293–2313. https://doi.org/10.1175/JHM-D-13-0196.1

Viviroli, D., Dürr, H. H., Messerli, B., Meybeck, M., & Weingartner, R. (2007). Mountains of the world, water towers for humanity: Typology, mapping, and global significance. *Water Resources Research*, *43*(7). https://doi.org/10.1029/2006WR005653

Wang, X., Tolksdorf, V., Otto, M., & Scherer, D. (2020). WRF-based dynamical downscaling of ERA5 reanalysis data for High Mountain Asia: Towards a new version of the High Asia Refined analysis. *International Journal of Climatology*, *41*(1), 743–762. https://doi.org/10.1002/joc.6686

Wrzesien, M. L., Pavelsky, T. M., Durand, M. T., Dozier, J., & Lundquist, J. D. (2019). Characterizing Biases in Mountain Snow Accumulation From Global Data Sets. *Water Resources Research*, *55*(11), 9873–9891. https://doi.org/10.1029/2019WR025350

Xiao, L., Che, T., & Dai, L. (2020). Evaluation of Remote Sensing and Reanalysis Snow Depth Datasets over the Northern Hemisphere during 1980–2016. *Remote Sensing*, *12*(19). https://doi.org/10.3390/rs12193253

Xu, Y., Jones, A., & Rhoades, A. (2019). A quantitative method to decompose SWE differences between regional climate models and reanalysis datasets. *Scientific Reports*, *9*(1), 16520. https://doi.org/10.1038/s41598-019-52880-5

Yao, T., Thompson, L., Yang, W., Yu, W., Gao, Y., Guo, X., Yang, X., Duan, K., Zhao, H., Xu, B., Pu, J., Lu, A., Xiang, Y., Kattel, D. B., & Joswiak, D. (2012). Different glacier status with atmospheric circulations in Tibetan Plateau and surroundings. *Nature Climate Change*, *2*(9), 663–667. https://doi.org/10.1038/nclimate1580

References from the supporting information

Bian, Q., Xu, Z., Zhao, L., Zhang, Y.-F., Zheng, H., Shi, C., Zhang, S., Xie, C., & Yang, Z.-L. (2019). Evaluation and Intercomparison of Multiple Snow Water Equivalent Products over the Tibetan Plateau. *Journal of Hydrometeorology*, *20*(10), 2043–2055. https://doi.org/10.1175/JHM-D-19-0011.1

Cho, E., Vuyovich, C. M., Kumar, S. V., Wrzesien, M. L., Kim, R. S., & Jacobs, J. M. (2022). Precipitation Biases and Snow Physics Limitations Drive the Uncertainties in Macroscale Modeled Snow Water Equivalent. *Hydrology and Earth System Sciences Discussions*, *2022*, 1–22. https://doi.org/10.5194/hess-2022-136

Clark, M. P., Hendrikx, J., Slater, A. G., Kavetski, D., Anderson, B., Cullen, N. J., Kerr, T., Örn Hreinsson, E., & Woods, R. A. (2011). Representing spatial variability of snow water equivalent in hydrologic and land-surface models: A review. *Water Resources Research*, *47*(7). https://doi.org/10.1029/2011WR010745

Gelaro, R., McCarty, W., Suárez, M. J., Todling, R., Molod, A., Takacs, L., Randles, C. A., Darmenov, A., Bosilovich, M. G., Reichle, R., Wargan, K., Coy, L., Cullather, R., Draper, C., Akella, S., Buchard, V., Conaty, A., da Silva, A. M., Gu, W., … Zhao, B. (2017). The Modern-Era Retrospective Analysis for Research and Applications, Version 2 (MERRA-2). *Journal of Climate*, *30*(14), 5419–5454. https://doi.org/10.1175/JCLI-D-16-0758.1

Hersbach, H., Bell, B., Berrisford, P., Hirahara, S., Horányi, A., Muñoz-Sabater, J., Nicolas, J., Peubey, C., Radu, R., Schepers, D., Simmons, A., Soci, C., Abdalla, S., Abellan, X., Balsamo, G., Bechtold, P., Biavati, G., Bidlot, J., Bonavita, M., … Thépaut, J.-N. (2020). The ERA5 global reanalysis. *Quarterly Journal of the Royal Meteorological Society*, *146*(730), 1999–2049. https://doi.org/10.1002/qj.3803

KOBAYASHI, S., OTA, Y., HARADA, Y., EBITA, A., MORIYA, M., ONODA, H., ONOGI, K., KAMAHORI, H., KOBAYASHI, C., ENDO, H., MIYAOKA, K., & TAKAHASHI, K. (2015). The JRA-55 Reanalysis: General Specifications and Basic Characteristics. *Journal of the Meteorological Society of Japan. Ser. II*, *93*(1), 5–48. https://doi.org/10.2151/jmsj.2015-001

Liu, Y., Fang, Y., & Margulis, S.A. (2021a). High Mountain Asia UCLA Daily Snow Reanalysis, Version 1. Boulder, Colorado USA, NASA Snow and Ice Data Center Distributed Active Archive Center. https://doi.org/10.5067/HNAUGJQXSCVU

Liu, Y., Fang, Y., & Margulis, S. A. (2021b). Spatiotemporal distribution of seasonal snow water equivalent in High Mountain Asia from an 18-year Landsat–MODIS era snow reanalysis dataset. *The Cryosphere*, *15*(11), 5261–5280. https://doi.org/10.5194/tc-15-5261-2021

Magnusson, J., Wever, N., Essery, R., Helbig, N., Winstral, A., & Jonas, T. (2015). Evaluating snow models with varying process representations for hydrological applications. *Water Resources Research*, *51*(4), 2707–2723. https://doi.org/10.1002/2014WR016498

Muñoz-Sabater, J., Dutra, E., Agustí-Panareda, A., Albergel, C., Arduini, G., Balsamo, G., Boussetta, S., Choulga, M., Harrigan, S., Hersbach, H., Martens, B., Miralles, D. G., Piles, M., Rodríguez-Fernández, N. J., Zsoter, E., Buontempo, C., & Thépaut, J.-N. (2021). ERA5-Land: A state-of-the-art global reanalysis dataset for land applications. *Earth System Science Data*, *13*(9), 4349–4383. https://doi.org/10.5194/essd-13-4349-2021

ONOGI, K., TSUTSUI, J., KOIDE, H., SAKAMOTO, M., KOBAYASHI, S., HATSUSHIKA, H., MATSUMOTO, T., YAMAZAKI, N., KAMAHORI, H., TAKAHASHI, K., KADOKURA, S., WADA, K., KATO, K., OYAMA, R., OSE, T., MANNOJI, N., & TAIRA, R. (2007). The JRA-25 Reanalysis. *気象集誌. 第 2 輯*, *85*(3), 369–432. https://doi.org/10.2151/jmsj.85.369

Petersky, R., & Harpold, A. (2018). Now you see it, now you don't: A case study of ephemeral snowpacks and soil moisture response in the Great Basin, USA. *Hydrology and Earth System Sciences*, *22*(9), 4891–4906. https://doi.org/10.5194/hess-22-4891-2018

Reichle, R. H., Draper, C. S., Liu, Q., Girotto, M., Mahanama, S. P. P., Koster, R. D., & De Lannoy, G. J. M. (2017). Assessment of MERRA-2 Land Surface Hydrology Estimates. *Journal of Climate*, *30*(8), 2937–2960. https://doi.org/10.1175/JCLI-D-16-0720.1

Rodell, M., Houser, P. R., Jambor, U., Gottschalck, J., Mitchell, K., Meng, C.-J., Arsenault, K., Cosgrove, B., Radakovich, J., Bosilovich, M., Entin, J. K., Walker, J. P., Lohmann, D., & Toll, D. (2004). The Global Land Data Assimilation System. *Bulletin of the American Meteorological Society*, *85*(3), 381–394. https://doi.org/10.1175/BAMS-85-3-381

Sturm, M., Holmgren, J., & Liston, G. E. (1995). A Seasonal Snow Cover Classification System for Local to Global Applications. *Journal of Climate*, *8*(5), 1261–1283. https://doi.org/10.1175/1520-0442(1995)008<1261:ASSCCS>2.0.CO;2

Wrzesien, M. L., Pavelsky, T. M., Durand, M. T., Dozier, J., & Lundquist, J. D. (2019). Characterizing Biases in Mountain Snow Accumulation From Global Data Sets. *Water Resources Research*, *55*(11), 9873–9891. https://doi.org/10.1029/2019WR025350

Xu, Y., Jones, A., & Rhoades, A. (2019). A quantitative method to decompose SWE differences between regional climate models and reanalysis datasets. *Scientific Reports*, *9*(1), 16520. https://doi.org/10.1038/s41598-019-52880-5